J Mater Sci (2010) 45:4507–4517
DOI 10.1007/s10853-010-4546-9

Effect of high temperature exposure on the microstructure of Udimet-500 super alloy

Noveed Ejaz · Muhammad Mansoor · Iftikhar Salam

Received: 23 November 2009 / Accepted: 21 April 2010 / Published online: 11 May 2010

Abstract Udimet-500 alloy is a high-strength nickel-bases super alloy used for turbine blades applications. It is primarily strengthened by very fine precipitates called gamma prime (γ') which coarsened with time when exposed to high temperature. In this study, Udimet-500 alloy in the standard aged condition was exposed at 850–1100 °C for 25–100 h in air. The change in the size of γ' with respect to the high temperature exposure was characterized using scanning electron microscope. A systematic coarsening of the γ' was observed with the change in the exposure temperature/time. The γ' size in the virgin sample was 0.1 μm while after high temperature exposures it coarsened to 1 μm. The Larson-Miller parameter (LMP) of the high temperature exposure was also measured. It was found that the LMP had power relation with the γ' size. In addition, degradation of the primary as well as secondary carbides was also observed which can be used as add-on microstructural information in high temperature exposure. Elevated temperature exposure (≥1000 °C) also lead to (a) near surface de-alloying, (b) precipitation of needle-like Ti-rich phase and (c) depletion of γ'. It may contribute in the accelerated corrosion and loss of strength of alloy.

Introduction

Udimet-500 alloy is a high-strength nickel-based super alloy used for turbine blades applications. It is strengthened primarily by very fine precipitates called γ', which coarsen with time when exposed to high temperature. If the coarsening of γ' is characterized at various temperatures, it could be used to evaluate the temperature experienced by the blades during service [1].

Earlier, many researches have quoted similar work for various super alloys. For example, Lvova and Norsworthy [2] and Cheruvu [3] have studied the influence of service conditions on microstructural changes in IN-738 and GTD-111, respectively. Similarly, Huff and Pillhofer [4] have quantitatively evaluated a relation between microstructural changes and exposure temperature in IN-100 alloy.

Premature failures of the Udimet-500 high pressure turbine blades have been reported due to microstructural degradation [5]. The γ' coarsening was the primary observation in it. The operational variations in the fighter aircraft engine may impart/induce temperature, higher than the service temperature in the turbine region. It consequently may lead to the catastrophic failure(s). The study of the microstructural variations with temperature/time may be useful in predicting service temperature. Afterward, during some intermediate overhaul, microstructural inspection of a blade of high-pressure region may be sufficient to avoid big accident.

Degradation of blades by high temperature exposures may also be imparted by other microstructural variations. It includes degradation of carbides and formation of deleterious phases. This information can be used additionally as a support to conclusion. Such microstructural variations have also studied and explained in this article.

With the prior knowledge of high temperature exposure and resultant microstructural degradation, the most of the properties suffered from high temperature exposure may be restored by an appropriate heat treatment accompanied by hot isostatic pressing [6, 7].

N. Ejaz (✉) · M. Mansoor · I. Salam
Institute of Industrial Control Systems,
P.O. Box 1398, Rawalpindi, Pakistan
e-mail: noveedejaz@yahoo.com

Experimental procedure and results

The study was carried out to simulate the over temperature conditions of the turbine blades of a fighter aircraft having two stage turbine, i.e. low- and high-pressure stages. In both stages, the material of the turbine blades was similar. They were manufactured through hot closed die forging process. The temperature in the low- and high-pressure turbine stages was ~700 and ~800 °C, respectively. A standard heat treatment was applied to the test specimens of UDIMET-500 to get a required initial microstructure. Subsequently, the effects of high temperature exposures for long as well as short durations on initial microstructure were studied. Scanning electron microscope (SEM) was used to characterize the microstructural features. In proceeding sections, experimental procedures and results are discussed.

Material chemistry

The analysis of the material was carried out using energy dispersive spectroscopy (EDS), combustion-type carbon sulphur (C/S) analyser and inductively coupled plasma. The results of analysis and standard alloy composition are given in Table 1.

Heat treatments

More than one heat treatment cycles for the Udimet-500 alloy are available in the literature [8, 9]. The heat treatment used to develop initial microstructure for test specimens is given in Table 2. The treatment caused fine distribution of γ' precipitates in the matrix (see Fig. 1). The resultant microstructure was also compared to that of airfoil of new turbine blade and found to be equivalent, showing that the initial specimens were bearing same metallurgical features as that of the original equipment manufacturer.

Table 1 Chemical composition of test sample(s) (wt%)

Element	Sample	Standard Udimet-500
C	0.07 ± 0.01	0.08
Cr	18 ± 0.5	18.0
Co	18 ± 0.5	18.5
Mo	3.8 ± 0.2	4
Ti	2.7 ± 0.2	2.9
Al	3.0 ± 0.2	2.9
B	<0.01	0.006
Zr	≤0.04	0.05
Ni	Bal.	Bal.

Table 2 Heat treatment cycle for alloy Udimet-500

#	Treatment	Temperature (°C)	Time (h)	Cooling media
1	Solution	1080	4	Air
2	Primary ageing	845	24	–
3	Secondary ageing	760	16	–

General microstructure of Udimet-500 alloy

Optical micrograph in Fig. 2 shows the general microstructure of a high-pressure turbine blade after 1,000 operating hours. Due to being used blade, the γ' was coarsened and resolved at low magnification. The microstructure shows (1) very fine globular γ', (2) faceted and irregular shaped primary carbides present mostly within the grains, (3) fine irregular shaped secondary carbides present at the grain boundaries.

High temperature exposures

The service temperature of the blades in the turbine region of the aircraft was in the range 750–800 °C. In order to reproduce the over temperature effects, 850 °C was selected as an initial exposure temperature. The long-term thermal exposures were conducted up to 1050 °C with an increment of 50 °C with primarily four exposure durations which is 25, 50, 75 and 100 h. Whereas, short-term thermal exposures for 5 and 30 min were also conducted at 1050, 1060 and 1070 °C.

Microscopy

The heat-treated specimens were prepared for metallography. Specimens were polished up to 0.05 μm grit and then etched. Two etching methods were used to reveal distinct microstructural details.

1. Electrolytically etched in 1.5% H_2CrO_4 solution at 6 V/1–5 s with stainless steel cathode.
2. Swab etching using Marble's reagent.

The former was found suitable for the study of size and morphology of γ' precipitates as the γ' precipitates remain in relief in this solution and the latter was suitable to study other features such as carbides. In this solution, the γ' precipitates etched out leaving recesses behind.

Subsequently, the etched samples were studied using SEM. In order to compare the change in size and morphology of the γ' precipitates after different exposures the micrographs were taken at 10000× magnification.

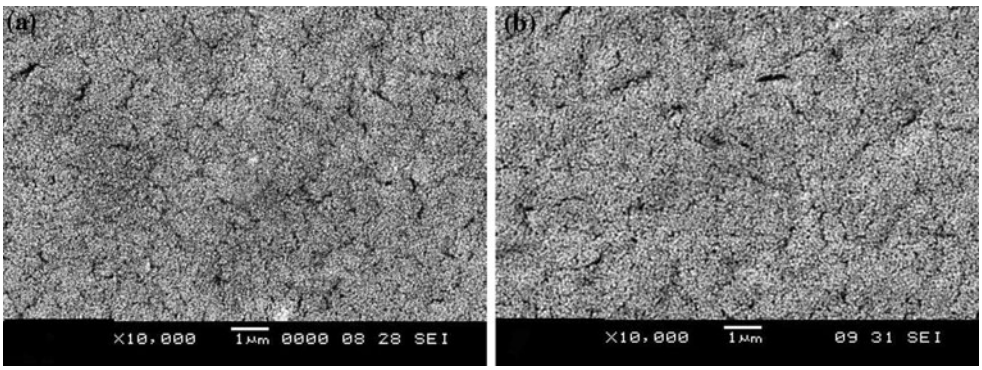

Fig. 1 Gamma prime in **a** new blade sample, **b** a sample solution treated at 1080 °C/4 h/AC, primary aged at 845 °C/24 h/AC, secondary aged at 760 °C/16 h/AC

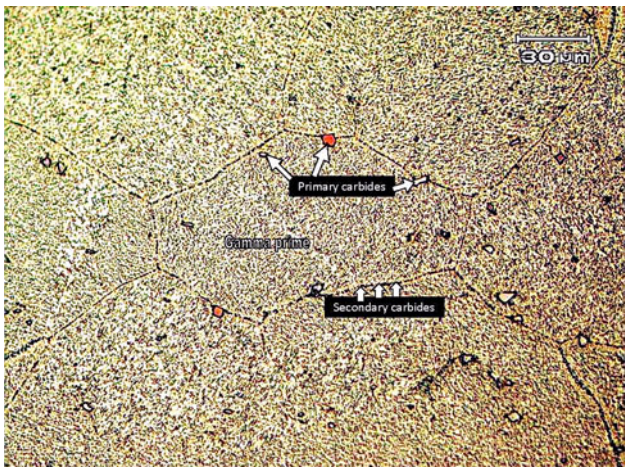

Fig. 2 The microstructure of the Udimet-500 alloy aged 700 h at 900 °C comprising of gamma prime (*fine dots*), faceted and irregular shaped primary carbides (MC type—*arrows* pointed out the same); very fine secondary carbides ($M_{23}C_6$ type) are also present on the grain boundaries

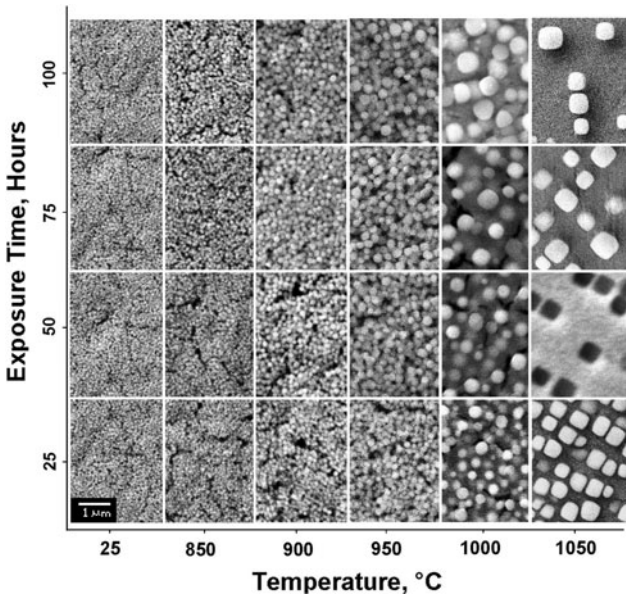

Fig. 3 SEM micrographs showing variation in the gamma prime size with temperature at different exposures; all micrographs are taken at 10000×

Size and morphology of γ′ precipitates

Figure 3 shows SEM micrographs of the γ' precipitates resulted after long duration exposures of the specimens at different temperatures and time. The effect of time and temperature on the size of γ' precipitates is evident. The size of the γ' increased with temperature and exposure time.

Morphology of the γ' precipitates remains globular up to 1000 °C while the size increases. In samples which were exposed to 1050 °C, the shape of the γ' precipitates was changed from globular to cubic (see Fig. 3). The percentage of γ' precipitates also decreases with increasing exposure time.

In the specimens exposed at 1050 °C, other shapes of γ' precipitates such as triangular (see Fig. 4a) and rectangular (see Fig. 4b) were also observed. These triangular and rectangular γ' precipitates were confined to few grains. It could be due to variation in the orientation of the γ' precipitates at the surface. Figure 4c schematically describes the orientation of the γ' precipitates just below the etched surface. The expected shape on the etched surface is also shown in the figure as well. In this regard such shapes may not be necessarily considered for size measurements.

Figure 5a, b shows the γ' precipitates after heat treatment at 1050 °C for 5 and 30 min, respectively, whereas Fig. 6a, b shows the same after heat treatment at 1060 °C for 5 and 30 min, respectively. In both cases, the coarsening of the γ' precipitates was observed but the shape was remained globular up to 30 min exposures. In contrast, at 1050 °C temperature and higher exposure time (25–100 h) the shape of the γ' precipitates was observed to be cubical. Although the size of the γ' was closer in either case of 1050

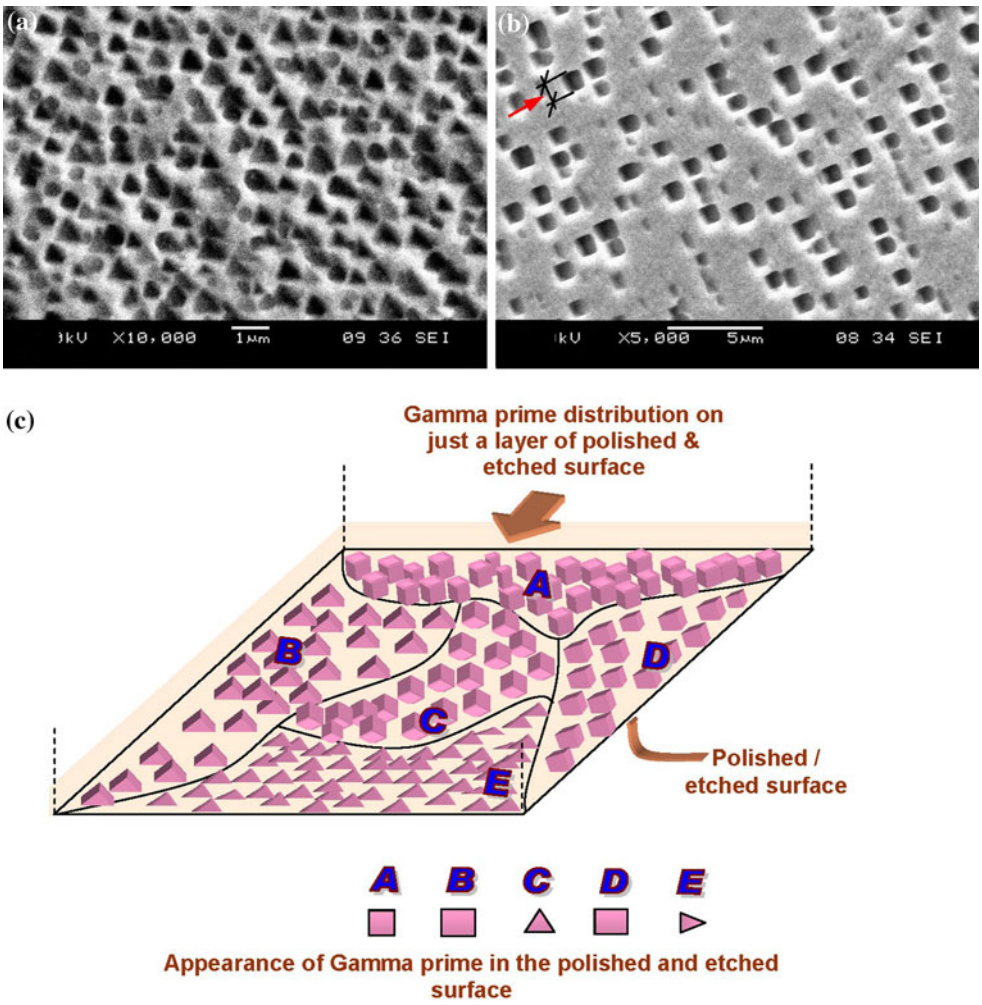

Fig. 4 Gamma prime after heat treatment at 1050 °C for **a** 25 h, **b** 100 h, **c** schematic showing the distribution and corresponding appearance of the gamma prime just below etched surface

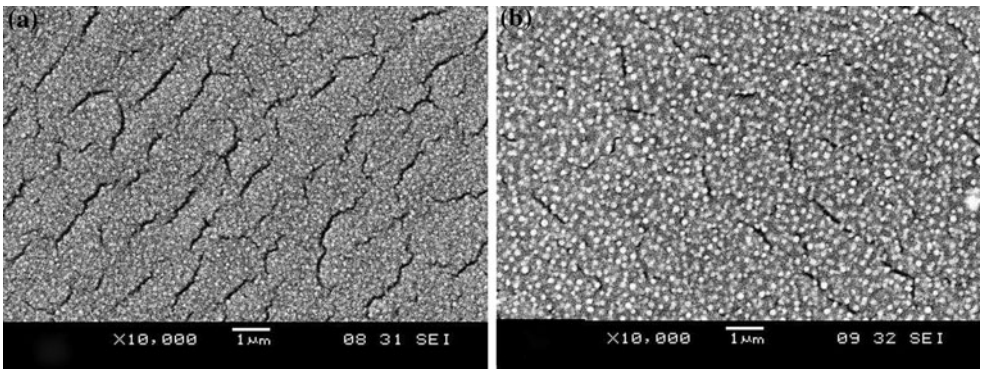

Fig. 5 Gamma prime after heat treatment at 1050 °C for **a** 5 min, **b** 30 min; *cracks* in the figures are only artefacts produced due to etchant

and 1060 °C exposure for 30 min, but the density of the γ' was seemed to be comparatively lower in the 1060 °C exposed sample. In the sample treated at 1060 °C a decrease in the percentage of γ' precipitates was observed as compared to the sample treated at 1050 °C for the same time, i.e. 30 min (see Fig. 6). The γ' disappeared at/above 1070 °C exposures.

An image analyser was used to measure the size of γ' precipitates. Figure 7a, b represents the plots of the variation in the size of γ' precipitates with temperature and time. A trend of gradual coarsening of γ' was observed. In the samples treated at 1070 °C the γ' precipitates were not observed; in the graph, the lines are extended (in dotted format) up to 1070 °C and dropped close to zero.

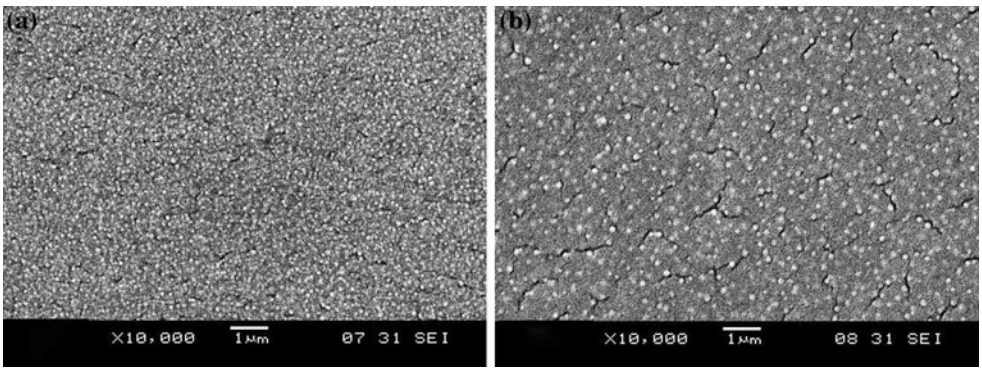

Fig. 6 Gamma prime after heat treatment at 1060 °C for **a** 5 min, **b** 30 min

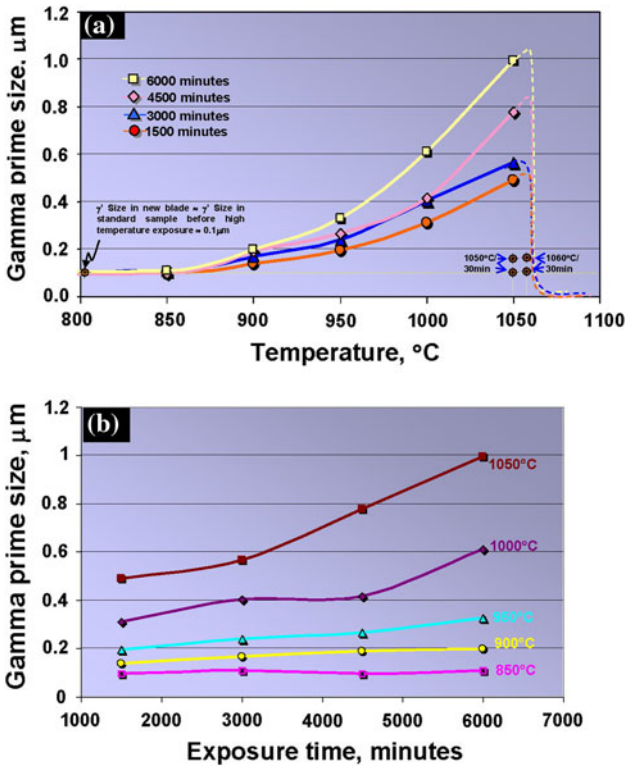

Fig. 7 Graph showing variation in the gamma prime size with **a** temperature for different exposure times, **b** time for different exposure temperatures

Use of Larson-Miller parameter Larson-Miller parameter (LMP) is one of the most commonly used combined time–temperature parameters applied for high-temperature degradation in the super alloys. The equation of the same is

$$\mathrm{LMP} = T \times [C + \log t] \tag{1}$$

where T is temperature in K and t is exposure time in hours; C is a constant which is usually in the range 20–25 for metals [10, 11].

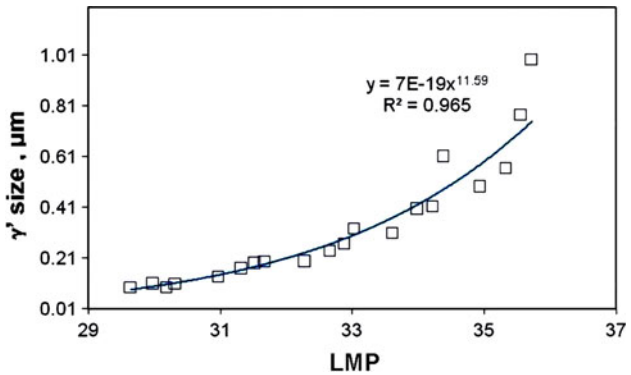

Fig. 8 Graph showing variation in the gamma prime size (γ'_s) with LMP exposure parameter

The LMP was also calculated and correlated with the γ' coarsening; the value of the constant C was substituted by 25 [11]. The results are presented in Fig. 8. The equation of closely fit line of the data was achieved with $R^2 \sim 0.965$ and is given below

$$\gamma'_s = 7 \times 10^{-19} \times (\mathrm{LMP})^{11.6} \tag{2}$$

where γ'_s is gamma prime size in μm.

Effects of high temperature exposure on the carbides

Figures 9, 10, 11 and 12 show the behaviour of carbides during high temperature exposures. Figure 9 indicates that the degradation of the carbides (primary as well as secondary) had initiated at 850 °C. In the course of degradation primary carbides converted partially into secondary carbides and the grain boundary secondary carbides coalesced to form continuous film. This degradation increased up to 1050 °C for ≥25 h exposure (see Figs. 10–12). For longer exposure time >50 h at the same temperature no secondary carbides were observed (see Fig. 12c–e). Figure 12f shows the micrograph of the sample treated at 1080 °C revealing only primary carbides in the matrix.

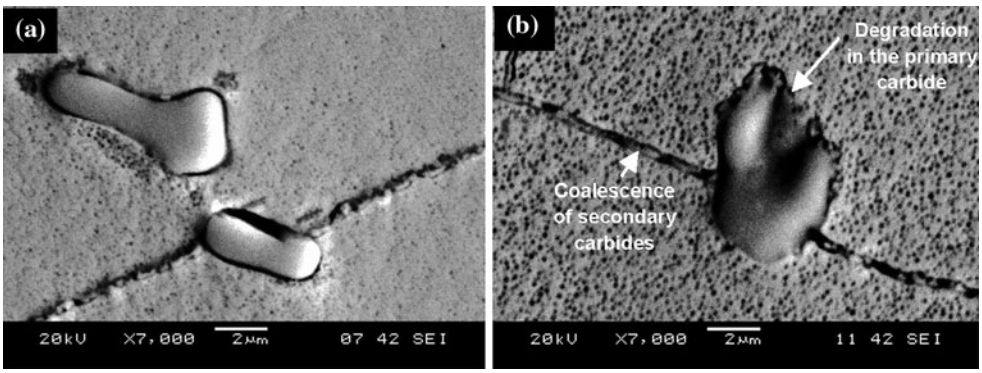

Fig. 9 **a** Primary and secondary carbides in the sample heat treated at 850 °C for 100 h. **b** Sample heat treated at 900 °C for 100 h; coalescence of secondary carbides and minor degradation in the primary carbide

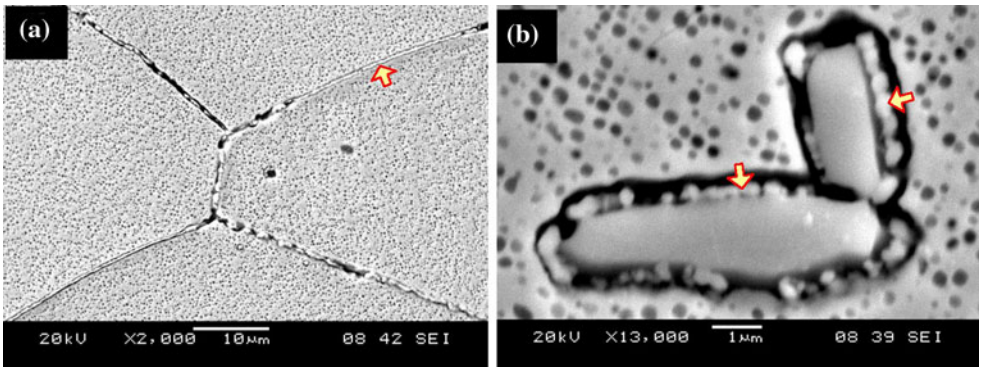

Fig. 10 Microstructure of sample heat treated at 950 °C for 100 h showing **a** coalescence of secondary carbides (*arrows*) and **b** degradation in the primary carbide (*arrows*)

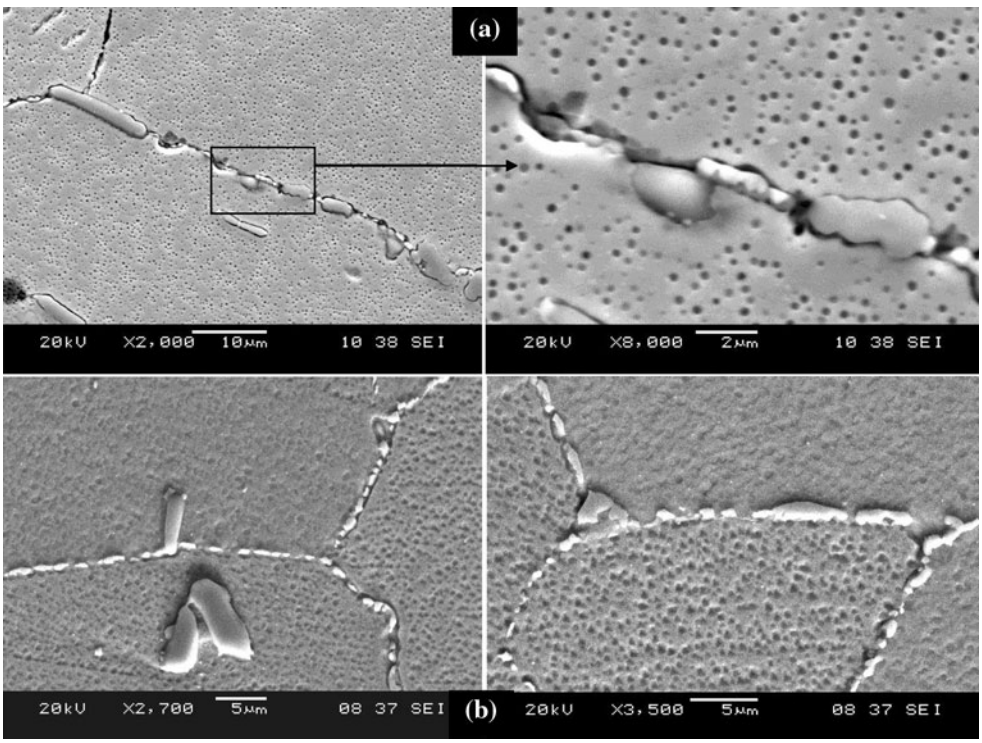

Fig. 11 Microstructure of samples heat treated at 1000 °C for **a** 25 h, **b** 100 h

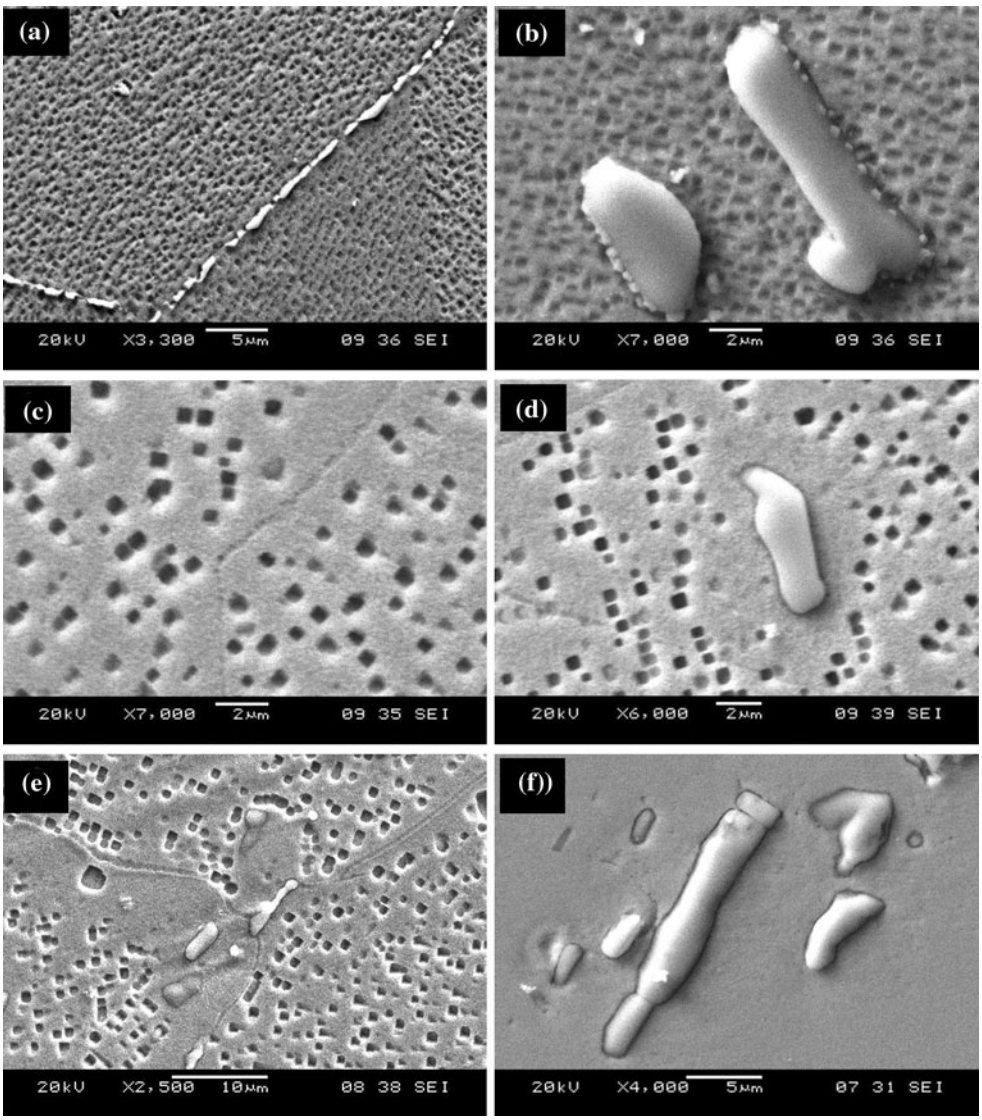

Fig. 12 Samples heat treated at 1050 °C for **a**, **b** 25 h, **c**, **d** 50 h and **e** for 100 h showing changes in the secondary and primary carbides; **f** treated at 1080 °C/25 h showing dissolution of secondary carbides as well as gamma prime

Near surface de-alloying

Besides the variation in the size and morphology of γ' precipitates and degradation of carbides, near surface de-alloying was also observed in the samples. The succession of the same is described below.

Titanium-rich phase was observed near the surface in samples treated at 1000 °C. Its morphology was irregular shaped after 25 h exposure which subsequently transformed into the needles-like shape after 75 h (see Fig. 13). After 100 h exposure, systematic growth in these needles was observed (see Fig. 14). The γ' precipitation was absent in this needle-like phase region (Fig. 14). Such features were also observed at 1050 °C/25 h exposure (see Fig. 15a). At this temperature, these needles were observed gradually disappeared when exposed for 50–100 h (see Fig. 15b–d).

Microprobe analysis of the needle-like phase and oxidation products were carried out using EDS equipped with the SEM. The results are given in Table 3. The locations of the analyses are marked in Fig. 16.

Discussion

Udimet-500 is a precipitation hardenable nickel base super alloy. The major phases present in this alloy are [12, 13] as follows.

1. Gamma (γ) phase is continuous FCC matrix composed of austenite. It is strengthened by the addition of solid

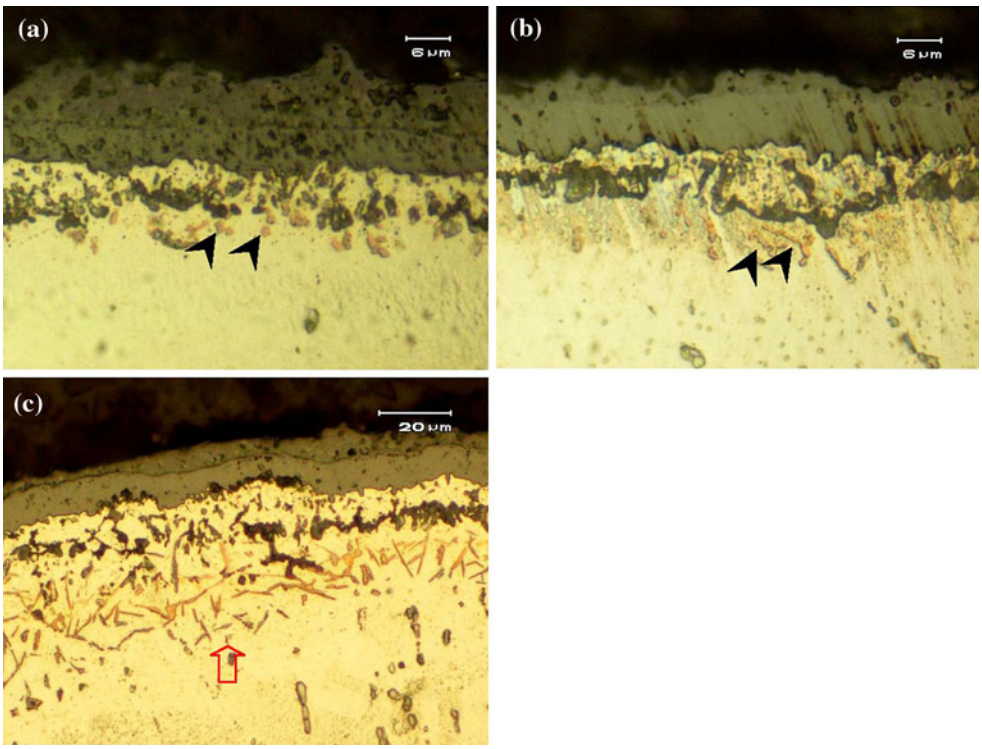

Fig. 13 Sample treated at 1000 °C for **a** 25, **b** 50 and **c** 75 h revealing growth of Ti-rich irregular shaped to needle-like phases near the surface (*arrows*)

solution elements such as chromium, molybdenum, cobalt, titanium and aluminium.

2. Gamma prime (γ') phase is the major precipitate phase. It is principally Ni_3Al or $Ni_3(Al,Ti)$. The lattice parameters of the γ are closer to γ', resulting in the coherency. The γ' is a major strengthening agent in the alloy.
3. Carbides are of various types in Ni-based super alloys. In case of Udimet-500, primary MC and secondary $M_{23}C_6$-type carbides are usually present in the alloy, where "M" stands for the metallic elements.

In MC carbides 'M' is usually titanium. Ti may partially be replaced by Mo in the carbide(s). These carbides are very stable and are believed to be formed just below the temperature where solidification begins.

In $M_{23}C_6$ carbides, 'M' is usually chromium, but this element can be replaced by molybdenum. $M_{23}C_6$ carbides are formed during lower-temperature heat treatments and in service within the temperature range 760–980 °C. They can also be formed by the dissociation of MC carbides as a result of the following reaction,

$$\gamma + \mathrm{MC} \rightarrow \mathrm{M_{23}C_6} + \gamma'$$

or

$$(\mathrm{Ni,\ Cr,\ Al,\ Ti}) + \mathrm{Ti(Mo)C} \rightarrow \mathrm{Cr_{23}Mo_2C_6} + \mathrm{Ni_3(Al,\ Ti)}$$

In precipitation hardenable nickel base super alloy, during long exposures at high temperatures, various microstructural changes may occur [8]; these could be

(a) γ' precipitates may coarsen and become over aged.
(b) γ' precipitates may also be elongated in the direction of loading (rafting).
(c) Grain boundary carbides may agglomerate to form continuous brittle film.
(d) Creep-induced cavities may also formed on grain boundaries, aligned normal to the stress axis.
(e) Brittle intermetallic phases such as sigma phase may also form.

In this study samples were given a standard heat treatment before starting the experiments of high temperature exposure. The microstructure of the standard samples was comparable with that of virgin blade. Samples were exposed up to 1080 °C for 25–100 h and 1050, 1060 and 1070 °C for 5 and 30 min, respectively. SEM of the etched specimens was used to detect high temperature effects on the microstructure of the Udimet-500 alloy (Fig. 3). Size of the γ' was increased systematically with temperature/exposure time. It was

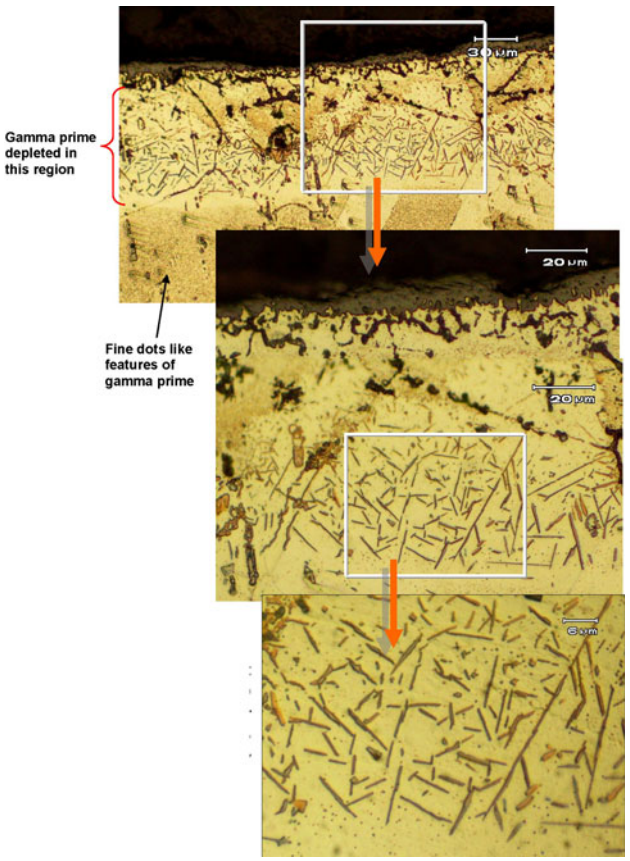

Fig. 14 Sample heat treated at 1000 °C for 100 h showing regular growth of phases into needle-like morphology

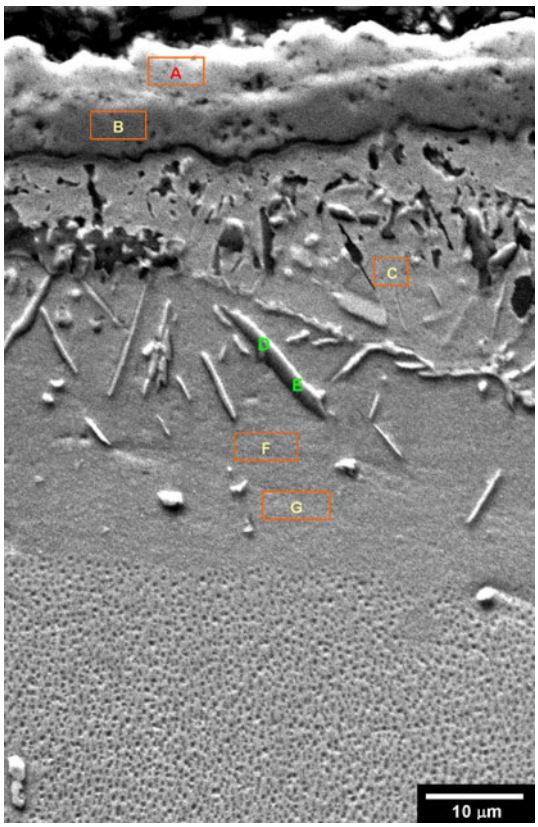

Fig. 16 Sample heat treated at 1050 °C for 25 h showing depletion zone and needle-like features near the surface

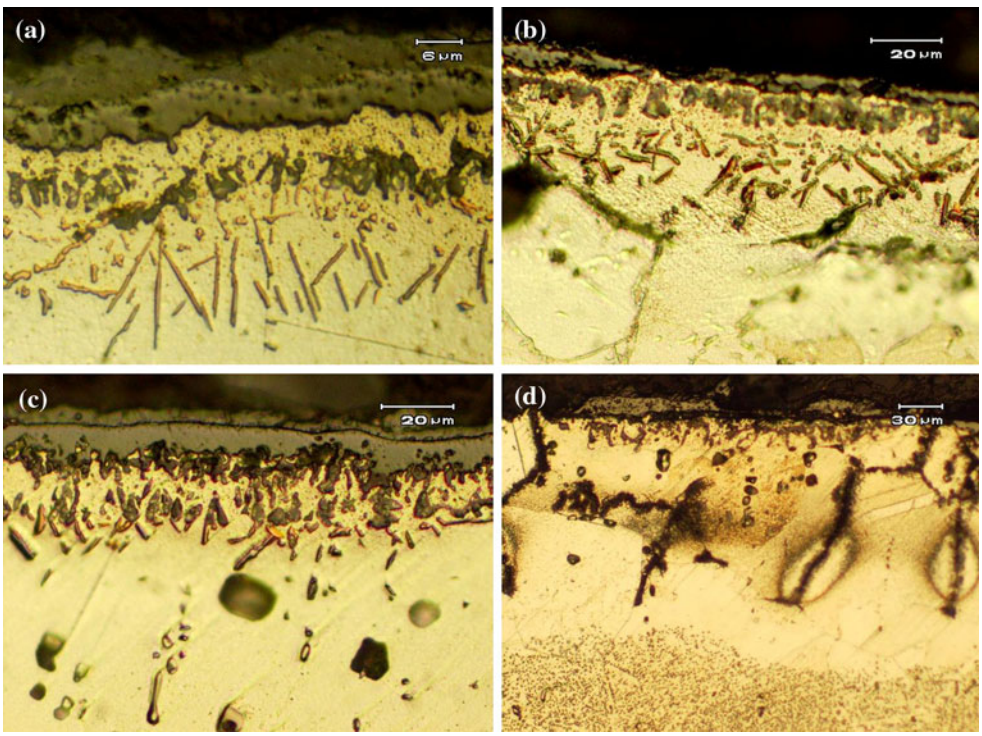

Fig. 15 Samples treated at 1050 °C for **a** 25, **b** 50, **c** 75 and **d** 100 h; note the change in the needle-like phase from **a** to **c**; these phase has vanished in **d**

Table 3 EDS analysis of phases/regions marked in Fig. 16

Region	Element (wt%)						
	Ni	Cr	Co	Mo	Ti	Al	O
A	13	29	18	–	7.5	2.5	Bal.
B	1.5	Bal.	0.38	0.5	3.32	1.76	30
C	Bal.	11	21	4.56	1.34	0.84	–
D	Bal.	13	15.8	4	22	0.9	–
E	Bal.	13	16	3	21	1.0	–
F	Bal.	17.9	19	2.5	1.7	1.8	–
G	Bal.	17.4	18.7	3.0	1.7	1.9	–

quantified by measuring the average diameter of the precipitates [14–16]. Figure 7a, b represents the graphical portray of the γ' size variation with temperature for different exposure times. The dotted lines were extrapolated to show the behaviour of the γ' precipitates size at higher temperatures. The initial size of the γ' was 0.1 μm, it verged onto 1 μm after 1050 °C exposure giving ten times growth. Additionally, the shape of the gamma prime was gradually transformed from globular to cubical. The change in the shape of γ' from globular to cuboidal is indicative of increase in the γ/γ' mismatch [17].

It was also observed that the density of the γ' precipitates visibly decreased with γ' growth at 1000 °C and onward (Fig. 3). The γ' size was observed closer in the samples treated at 1050 and 1060 °C for 5 and 30 min, respectively. Similar observations were noted in samples treated at both temperatures for 30 min. In contrast, the density of γ' was seemed to be comparatively lower in the samples treated at 1060 °C (see Figs. 5 and 6). It may be due to partial dissolution and growth of the γ' in the matrix. In this regards, the reaction of the primary carbides with the matrix-yielding secondary carbides might also play some role in the thermodynamics of the alloy promoting γ' coarsening.

LMP was also calculated and correlated with the variation in the γ' size. It is the exposure parameter which is indicative of the combined effects of the time and temperature. A comprehensive relation of LMP with γ' size (Eq. 2) has been derived using a software. The regression $R^2 \approx 0.965$ was achieved indicating soundness of the resultant with γ' size.

The transformation of the primary carbides (usually Ti(Mo)C) [18] to secondary carbides (usually $Cr_{21}Mo_2C_6$) [18] and coalescence of secondary carbides at the grain boundaries were observed at temperature up to 950 °C for 100 h and at 1050 °C for 25 h (see Figs. 9–12). At 1050 °C and above the secondary carbides were completely disappeared. Probably they could be dissolved in the solution.

Needle-like phases were also observed near the surface regions in the samples exposed to 1000 °C; it gradually disappeared at 1050 °C. EDS analysis revealed that they were rich in titanium (Fig. 16, Table 3). Their morphology was matching to sigma (σ) phase [7]. During high temperature exposures the reactive elements of the alloy such as Ti, Al and Cr diffused outward form inside the alloy, leaving depleted zone near the surface of alloy [19]. Due to change in composition at that region, the γ' formation was no longer favoured at this region (see Fig. 16).

Conclusions

- The γ' size in the virgin blade of Udimet-500 alloy was $\approx$0.1 μm while after high temperature exposures it coarsened to 1 μm. These ten times systematic increase in the γ' size can be utilized as a reference for the assessment of exposure temperature/time exceeding to the service temperature [20].
- The γ' size has a power relation with LMP. Thence the high temperature exposure can be predicted in terms of coarsening of γ'.
- The degradation of the carbides can be used as an add-on information in assessment of microstructural degradation at high temperature exposure.
- Elevated temperature exposure ($\geq$1000 °C) lead to (a) near surface de-alloying, (b) precipitation of needle-like Ti-rich phase and (c) depletion of γ'; it may bring about loss of strength and accelerated corrosion of the alloy.

References

1. Naga M, Kanaya A, Imano S, Doi H, Ichikawa K (2004) In: 16th world conference on NDT, Montreal, Canada, www.ndt.net
2. Lvova E, Norsworthy D (2001) J Mater Eng Perform 10(3):299
3. Cheruvu NS (2000) In: Proceeding of 2000 international joint power generation conference, Miami Beach, Florida, 23–26 July 2000, Paper IJPGC2000-15068
4. Huff H, Pillhofer H (1988) In: Superalloys 1988, The Metallurgical Society, pp 835–843

5. Ejaz N, Tauqire A (2006) Eng Fail Anal 13:452
6. Koul AK et al (1988) In: Reichman S (ed) Superalloys-1988. The Metallurgical Society, Inc., Warrendale, PA, p 755
7. James A (2001) Mater Sci Technol 17:481
8. Hunt MW (ed) (1999) ASM J Adv Mater Proc 156:79
9. Stolof CT, Norman S, Hagel WC (1987) Superalloys-II. Wiley, New York, pp 124–125
10. Hertzberg RW (1996) Deformation and fracture mechanics of engineering materials, 4th edn. Wiley, Hoboken, NJ
11. Wlodek ST, Field RD (1994) In: Loria EA (ed) Superalloy 718, 625, 706 and various derivatives. The Minerals Metals and Materials Research Society, pp 659–671
12. Smith WF (1993) Structure and properties of engineering alloys, 2nd edn. McGraw Hill, New York, p 47
13. Chester CS (1966) J Met 10:1119
14. Vander Voort GF (1986) In: Kathleen M, Davis JR (eds) Metallography and microstructure. Metal handbook, vol 9, 9th edn. ASM, Materials Park, OH, pp 305–329
15. Stolof CT, Norman S, Hagel WC (1987) Superalloys II. Wiley, New York, pp 124–125
16. Murphy HJ, Sims CT (1967) Trans AIME 239:1961
17. Loomis WT et al (1972) Met Trans 3:989
18. Sims CC (1966) J Met 18:1119
19. Lindblom Y (1978) In: Courtsouradis D et al (eds) Creep and structural stability of high temperature materials: high temperature alloys for gas turbines. Applied Science Publishers, England, pp 285–316
20. Metallurgical Analysis, Liburdi Engineering, Technology Update 1(2), 1996